Lattice study for the HLS-Ⅱ storage ring *

BAI Zheng-He(白正贺)[1)] WANG Lin(王琳)[2)] JIA Qi-Ka(贾启卡) LI Wei-Min(李为民)

National Synchrotron Radiation Laboratory, University of Science and Technology of China, Hefei 230029, China

Abstract: The Hefei Light Source (HLS) is undergoing a major upgrade project, named HLS-Ⅱ, in order to obtain lower emittance and more insertion device straight sections. Undulators are the main insertion devices in the HLS-Ⅱ storage ring. In this paper, based on the database of lattice parameters built for the HLS-Ⅱ storage ring obtained by the global scan method, we use the quantity related to the undulator radiation brightness to more directly search for high brightness lattices. Lattice solutions for achromatic and non-achromatic modes are easily found with lower emittance, smaller beta functions at the center of the insertion device straight sections and lower dispersion in non-zero dispersion straight sections compared with the previous lattice solutions. In this paper, the superperiod lattice with alternating high and low horizontal beta functions in long straight sections for the achromatic mode is studied using the multiobjective particle swarm optimization algorithm.

Key words: storage ring, lattice, undulator, brightness, emittance, particle swarm optimization

PACS: 29.20.db, 29.27.Bd **DOI:** 10.1088/1674-1137/37/4/047004

1 Introduction

The Hefei Light Source (HLS) is a second-generation light source in the VUV (vacuum ultraviolet) and soft X-ray regions and was the first dedicated synchrotron light source in China. It has been operating for more than 20 years, but now the present HLS cannot satisfy user requirements very well and has fallen behind its competitors around the world. Therefore, an upgrade plan to improve the performance of the HLS was proposed two years ago, and the corresponding upgrade project, named HLS-Ⅱ, is now underway.

In the upgrade plan, the energy and circumference of the storage ring remain at 800 MeV and about 66 m, respectively. In contrast to the present TBA (triple bend achromatic) lattice, the HLS-Ⅱ storage ring adopts a DBA (double bend achromatic) lattice, which can provide more available straight sections for insertion devices. The natural emittance can be reduced from the present 166 nm·rad to less than 40 nm·rad in the achromatic mode, and it is about 20 nm·rad in the non-achromatic mode. The magnet layout of the HLS-Ⅱ storage ring is shown in Fig. 1. The HLS-Ⅱ storage ring has four DBA cells, and each cell has a 4 m long straight section and a 2.3 m medium straight section. In addition to a long straight section for injection and a medium straight section for the RF cavity, the other straight sections can be used for the installation of insertion devices. In the present plan, two undulators will be installed in two long straight sections, and two undulators and one wiggler will be installed in three medium straight sections.

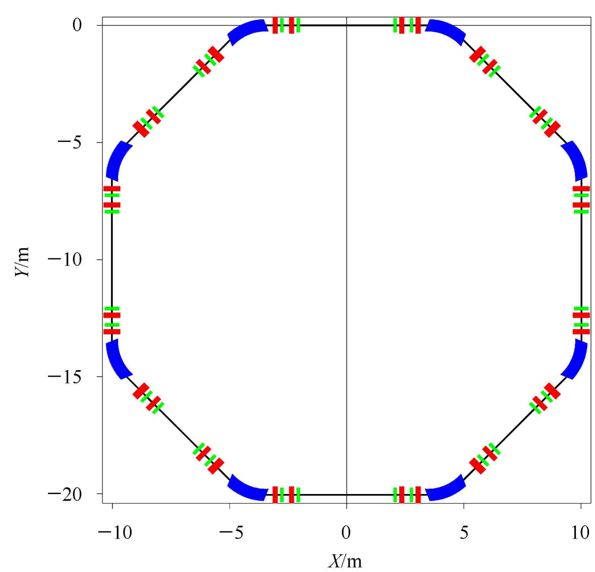

Fig. 1. (color online) The geometry of the magnet layout of the HLS-Ⅱ storage ring.

In this paper, we take the reciprocal of the phase space volume of the undulator radiation source as the

Received 9 May 2012

∗ Supported by National Natural Science Foundation of China (11175182, 10979045)

1) E-mail: baizheng@mail.ustc.edu.cn

2) E-mail: wanglin@ustc.edu.cn

object of the lattice study. This is related to the lattice parameters and proportional to the undulator radiation brightness. Thus, based on the built database of the HLS-Ⅱ storage ring lattice parameters obtained by the global scan method, we can easily find high-brightness lattice solutions for both the achromatic and non-achromatic modes. Besides, to lower the horizontal beta function in long straight sections for insertion devices in the achromatic mode, the case of two-superperiod lattice with alternating high and low horizontal beta functions in long straight sections is studied using the multiobjective particle swarm optimization algorithm.

2 Brightness-related lattice study

The undulator radiation brightness is defined as the photon flux per unit phase space volume, in units of photons/(s×0.1%bandwidth×mm^2×mrad^2), and for Gaussian beam distribution is given by

$$B=\frac{F_n}{4\pi^2\sigma_{Tx}\sigma_{Ty}\sigma_{Tx'}\sigma_{Ty'}}, \tag{1}$$

where F_n is the photon flux, and the denominator is the phase space volume of the photon source (usually at the center of the undulator) given by the effective source sizes and effective source divergences in the horizontal and vertical planes. The effective source size σ_{Tu} and divergence $\sigma_{Tu'}$ ($u=x$ for the horizontal plane and $u=y$ for the vertical) are the results of the convolution of the electron beam and diffraction limited photon beam parameters:

$$\sigma_{Tu}=\sqrt{\sigma_u^2+\sigma_r^2},\quad \sigma_{Tu'}=\sqrt{\sigma_{u'}^2+\sigma_{r'}^2}, \tag{2}$$

with σ_u and $\sigma_{u'}$, respectively, the electron beam size and divergence, and σ_r and $\sigma_{r'}$, respectively, the diffraction limited photon beam size and divergence given by

$$\sigma_r=\frac{1}{2\pi}\sqrt{\frac{\lambda L}{2}},\quad \sigma_{r'}=\sqrt{\frac{\lambda}{2L}}, \tag{3}$$

where L is the undulator length and λ the radiation wavelength.

Usually, the linear optics of the electron beam is symmetrical with respect to the center of the undulator. In this case, the electron beam sizes and divergences at the center of the undulator in the horizontal and vertical planes are, respectively, given by

$$\sigma_x = \sqrt{\varepsilon_x\beta_x+\sigma_\delta^2\eta^2},\quad \sigma_{x'}=\sqrt{\frac{\varepsilon_x}{\beta_x}}, \tag{4}$$

$$\sigma_y = \sqrt{\varepsilon_y\beta_y},\quad \sigma_{y'}=\sqrt{\frac{\varepsilon_y}{\beta_y}}, \tag{5}$$

with β_x and β_y, respectively, the horizontal and vertical beta functions at the center of undulator, η the dispersion function at the center of the undulator, σ_δ the relative energy spread, and ε_x and ε_y, respectively, the horizontal and vertical emittances given by

$$\varepsilon_x=\frac{1}{1+\kappa}\varepsilon_{x0},\quad \varepsilon_y=\frac{\kappa}{1+\kappa}\varepsilon_{x0}, \tag{6}$$

where κ is the coupling ratio and ε_{x0} is the natural emittance.

In Eq. (1), the photon flux does not depend on the lattice parameters, while the phase space volume of the photon source is related to the lattice parameters. So in the lattice design, the solution to increasing brightness is to minimize the phase space volume of the photon source, i.e. to minimize σ_{Tu} and $\sigma_{Tu'}$ expressed by Eq. (2). From Eq. (3) to Eq. (6), we can easily see that the most efficient solution to increasing brightness is to reduce electron beam emittance. Besides, optimizing the beta functions at the center of the straight sections will also increase the brightness. To gain the maximum brightness, from Eq. (3) to Eq. (5) we can derive that in the zero-dispersion straight sections the optimal beta functions are [1]

$$\beta_{x,y}=\frac{L}{2\pi}, \tag{7}$$

and in the non-zero dispersion straight sections the optimal horizontal beta function is changed to [2]

$$\beta_x=\sqrt{\frac{2L}{\lambda}\sigma_\delta^2\eta^2+\frac{L^2}{4\pi^2}}. \tag{8}$$

In other words, at these beta values there is an optimal matching between the electron beam and diffraction limited photon beam phase spaces.

In contrast to optimizing the electron beam emittance and beta functions, to more directly search for lattice solutions with high brightness and to explore the potential of brightness enhancement of the HLS-Ⅱ storage ring, we take the reciprocal of the phase space volume of the photon source (at the center of the straight sections) $R_{\rm V}$

$$R_{\rm V}=\frac{1}{4\pi^2\sigma_{Tx}\sigma_{Ty}\sigma_{Tx'}\sigma_{Ty'}}, \tag{9}$$

as the object of the lattice study, which is proportional to the undulator brightness.

In our laboratory, the global scan method was applied to the lattice design of the HLS-Ⅱ storage ring [3], and the obtained data provided us with global solutions and their lattice parameters. Thus, for all the solutions of interest, we can directly use their lattice parameters to calculate $R_{\rm V}$ for long and medium straight sections in both the achromatic and non-achromatic modes. This calculation is also dependent on the undulator radiation wavelength. In our study, we choose a longer wavelength and a shorter wavelength in the wavelength range as the representative of the range, and for each chosen wavelength R_{V} is calculated for all the solutions of interest.

To calculate R_{V}, the undulator length and radiation wavelength values are determined according to the design of undulators for the HLS-II storage ring [4]. For simplicity, in our calculation the two undulators in long straight sections have the same length of 3 m, which is their average value, and similarly the two undulators in medium straights have the same length of 1.5 m. For the two undulators in long straights, 200 nm and 15 nm are taken as the longer and shorter wavelength values, respectively. And for the two undulators in medium straights, the longer and shorter wavelength values are, respectively, 150 nm and 10 nm. Besides, we set the coupling ratio to be 5%. A small coupling ratio is also a method often used to increase the brightness, though it may cause the problem of short beam lifetime. For the HLS-II storage ring, the coupling ratio would be reduced by two families of skew quadrupoles after the execution of a top-off injection scheme in the future.

There are four families of quadrupoles in the HLS-II storage ring. To obtain global information about the storage ring lattice, a global scan of quadrupole strengths has been conducted in the range $[-5\ \mathrm{m}^{-2}, 5\ \mathrm{m}^{-2}]$ with a grid spacing of $0.05\ \mathrm{m}^{-2}$. The obtained database of lattice solutions and parameters will be used for the following study.

To select the solutions of interest from the obtained solutions in the scan, we set the common requirements for both achromatic and non-achromatic lattices:

1) natural emittance <100 nm·rad;
2) maximum β_x, β_y<25 m;
3) maximum absolute dispersion <1.5 m;
4) β_x at the center of long straight >5 m;
5) β_y at the center of long straight <3 m;
6) β_y at the center of medium straight <3 m.

For the achromatic mode, two additional requirements are set. First, the absolute dispersion at the center of the long straight is set to be less than 0.1 m, which is roughly considered the achromatic condition. Second, the strength values of the two chromatic sextupoles used for correcting the natural chromaticities to zero are required to be less than 120 m^{-3}. And for the non-achromatic mode, the additional requirement is that the absolute dispersion at the center of the long straight is less than 0.8 m.

For the selected solutions of interest for the achromatic mode, according to their lattice parameters, R_{V} is calculated for the long straight section at wavelength values of 200 nm and 15 nm, and for the medium straight section at wavelength values of 150 nm and 10 nm. Fig. 2 shows the maximum values of R_{V} reached at different values of natural emittance. The left plot is for the long straight section, and the right plot for the medium straight section. These give a clear picture about the potential of brightness enhancement at the HLS-II storage ring. We can see that the lower the natural emittance is, the larger the value of R_{V} is reached, except for the case of the long straight section at a wavelength value of 200 nm. This is because β_x at the center of the long straight section becomes larger when electron beam emittance is reduced (see Fig. 6 in the next section). When electron beam emittance approaches the diffraction emittance (16 nm·rad for 200 nm), the beta function becomes important for matching between the electron beam and diffraction limited photon beam phase spaces.

Note that Fig. 2 only shows the maximum values of R_{V}, not the values of R_{V} for all solutions of interest. With the R_{V} values, we can easily discover high brightness achromatic lattices. To find the high brightness lattices, we relax the restriction of the fractional parts of the working point (i.e. the fractional parts can be larger than 0.5). Besides, we consider the quadrupole strength margin for correcting the linear optics perturbed by insertion devices. The nonlinear dynamics is also considered. The values of R_{V} for the long and medium straight sections

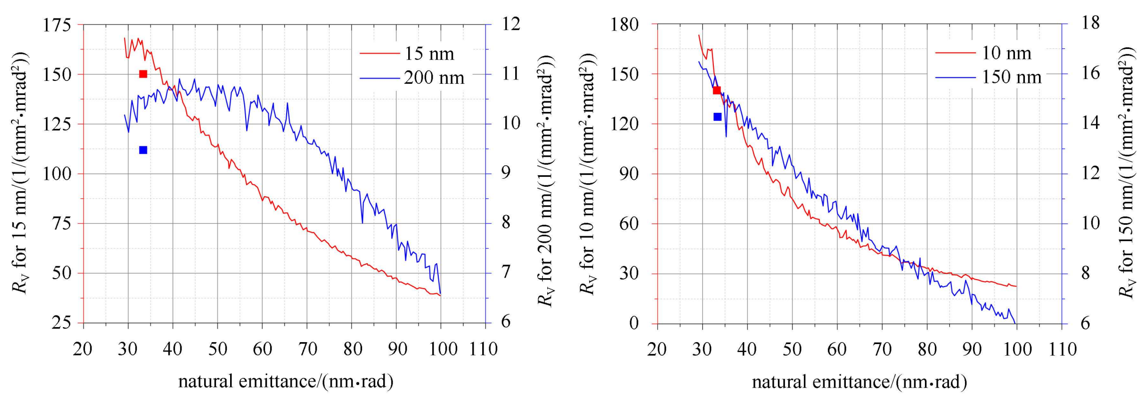

Fig. 2. (color online) The maximum values of R_{V} reached at different values of natural emittance (shown as curves), and the R_{V} values of one found lattice (shown as squares) for the achromatic mode (the left plot is for the long straight section and the right for the medium straight section).

of one found lattice are also shown in Fig. 2 (the red square represents the short wavelength and the blue square the long wavelength).

The optical functions of one period of the found achromatic lattice are shown in Fig. 3. The natural emittance is 33.4 nm·rad. The values of β_x and β_y at the center of the long straight section are, respectively, 17.44 m and 1.86 m, and β_x and β_y at the center of the medium straight section are, respectively, 2.34 m and 1.10 m. The dispersion function in the medium straight section is 0.78 m. All these lattice parameters are lower than those of the previous achromatic lattice [3]. The working point of this lattice is (4.616, 3.568), and the momentum compaction factor is 0.0205. In addition, the optimized dynamic aperture is large enough.

For the selected solutions of interest for the non-achromatic mode, according to their lattice parameters, $R_{\rm V}$ is also calculated for the long and medium straight sections. The maximum values of $R_{\rm V}$ reached at different natural emittance values are shown in Fig. 4, and the left and right plots are, respectively, for the long and medium straight sections. The $R_{\rm V}$ values for the long and medium straight sections of one found lattice are also shown in Fig. 4 (the red and blue squares represent, respectively, the short and long wavelengths).

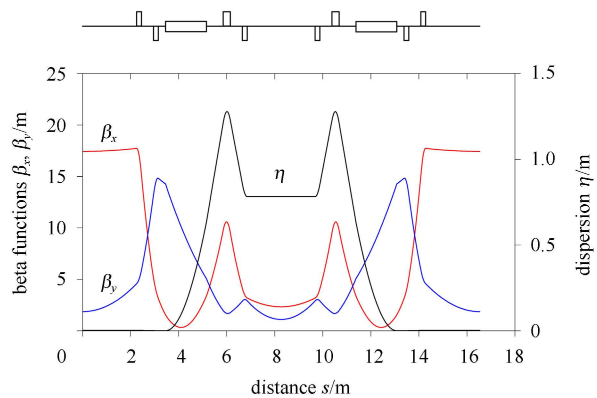

Fig. 3. (color online) The optical functions of one period for the achromatic mode.

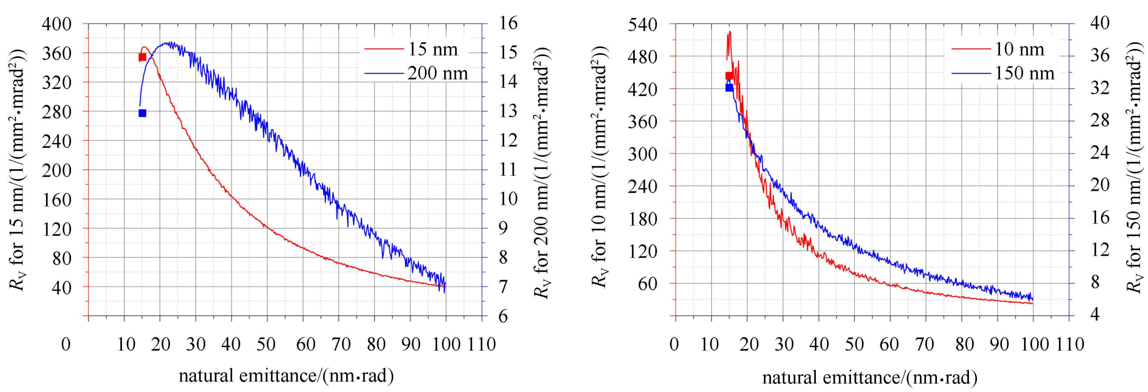

Fig. 4. (color online) The maximum values of $R_{\rm V}$ reached at different values of natural emittance (shown as curves), and the $R_{\rm V}$ values of one found lattice (shown as squares) for the non-achromatic mode (the left plot is for the long straight section and the right plot for the medium straight section).

The optical functions of one period of the found non-achromatic lattice are shown in Fig. 5. The natural emittance is 14.9 nm·rad, which is close to the lowest emittance 14.0 nm·rad found in the global scan. The values of β_x and β_y at the center of the long straight section are, respectively, 18.74 m and 0.88 m, and β_x and β_y at the center of the medium straight section are, respectively, 0.92 m and 0.90 m. Note that of these beta values, three are less than 1 m. The dispersion function in the medium straight section is 0.42 m, which is lower than that of the previous non-achromatic lattice [3]. The dispersion function in the long straight section is 0.77 m. The working point is (5.210, 3.727), and the momentum compaction factor is 0.0129. Additionally, the optimized dynamic aperture is also large enough.

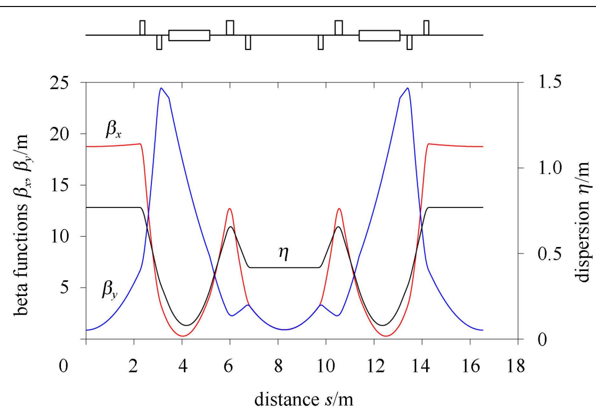

Fig. 5. (color online) The optical functions of one period for the non-achromatic mode.

Though the above lattice study is about undulator brightness enhancement, the lower emittances of the two found lattices also have a positive effect on bend magnet brightness, which is roughly inversely proportional to the natural emittance.

3 Superperiod lattice study

To reduce the effect of the elliptically polarizing undulator in the long straight section on emittance increase due to large linear optics perturbation, β_x at the center of the long straight section should be lowered. A lower β_x will also increase undulator brightness. A lower β_x may have little effect on injection because usually the optimized dynamic aperture of the HLS-II storage ring is large enough. We will study the possibility of lowering β_x at the center of the long straight section for the achromatic mode.

Figure 6 shows the values of natural emittance and β_x at the center of the long straight section of all the selected solutions of interest for the achromatic mode (discussed in the previous section). We can see that at low natural emittances the value of β_x at the center of the long straight section is large. This means that at low natural emittances there is no lattice solution with small β_x. So we turn to study the case of the superperiod lattice for the HLS-II storage ring, in which the four cells form two superperiods.

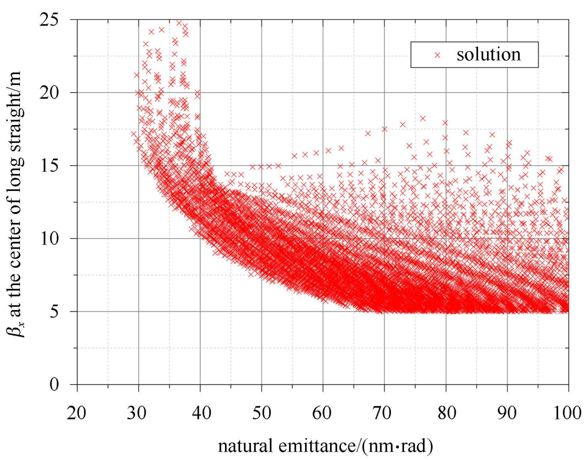

Fig. 6. (color online) The natural emittance and β_x at the center of the long straight section of all the selected solutions for the achromatic mode.

In this superperiod lattice, there are eight families of quadrupoles. So the global scan method cannot be applied due to huge computation, and the artificial intelligence algorithm is considered. Here we use the multiobjective particle swarm optimization (MOPSO) algorithm [5] to optimize these eight variables of quadrupole strength. The particle swarm optimization algorithm is a widely used artificial intelligence algorithm for global optimization. We set the following basic constraints for the superperiod lattice:

1) maximum β_x, β_y <30 m;

2) maximum absolute dispersion <2.0 m;

3) β_y at the center of the long and medium straights <4 m;

4) β_x at the center of the long straight (for the undulator) <6 m.

In this optimization, one objective is the natural emittance, and the other is the sum of two absolute dispersions in two long straights (for the injection and undulator, respectively). The MOPSO algorithm, with a population size of 100000 ran for 300 iterations, and the obtained Pareto optimal front is shown in Fig. 7. The Pareto optimal front is an image of a set of non-dominant solutions in objective space. In this optimization, we also set the two absolute dispersions in two long straights to be less than 0.5 to better consider the achromatic condition. Here, the achromatic condition for the superperiod lattice is where the two absolute dispersions in two long straights are zero. In Fig. 7, we can see that the lowest emittance of the achromatic superperiod lattice is about 55 nm·rad.

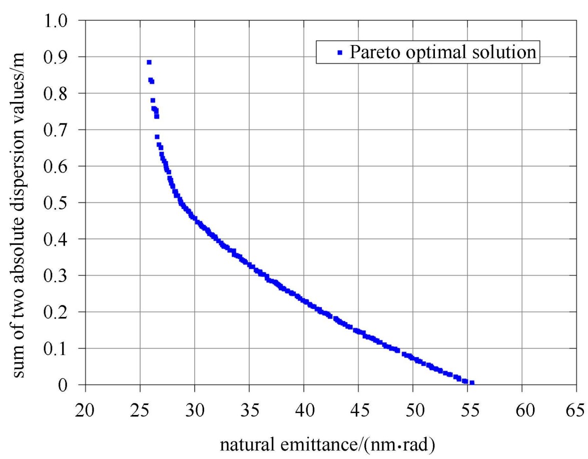

Fig. 7. (color online) The Pareto optimal front for the superperiod lattice.

The optical functions of one superperiod of one achromatic superperiod lattice are shown in Fig. 8, with alternating high and low horizontal beta functions in the long straight sections. The natural emittance of this two-superperiod lattice is 55 nm·rad, which is significantly larger than 33 nm·rad. In the case of the four-period lattice, at the natural emittance of 55 nm·rad, the lowest value of β_x at the center of the long straight is also close to 6 m, as shown in Fig. 6. So in the case of a two-superperiod lattice, there is also no lattice solution with both low natural emittance and small β_x at the center of the long straight (for the undulator). This means that the lattice flexibility of the HLS-Ⅱ storage ring is limited.

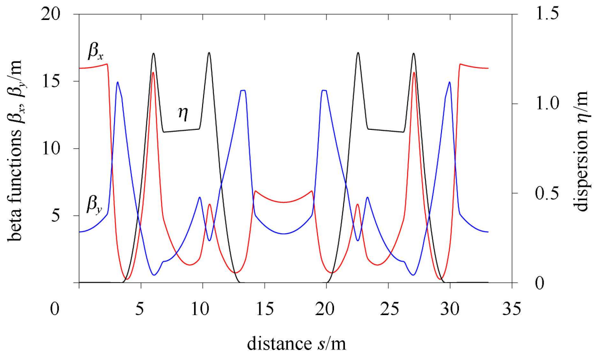

Fig. 8. (color online) The optical functions of one superperiod for the achromatic superperiod lattice.

4 Conclusions

We studied the cases of the high brightness lattice and the superperiod lattice for the HLS-Ⅱ storage ring. To more directly search for high brightness lattice solutions from the database of lattice solutions and the parameters obtained by the global scan method, the reciprocal of the phase space volume of the undulator radiation source is calculated for long and medium straight sections, which is proportional to undulator brightness. This calculation gives a clear picture of the potential of brightness enhancement at the HLS-Ⅱ storage ring. High brightness lattice solutions for both the achromatic and non-achromatic modes are easily found. To reduce the perturbation from the elliptically polarizing undulator in the long straight section on linear optics, the two-superperiod achromatic lattice with alternating high and low horizontal beta functions in the long straight sections was studied using the MOPSO algorithm. The results of the superperiod lattice study show that there is no ideal lattice solution with both low natural emittance and small β_x at the center of the long straight for the undulator due to the limited lattice flexibility of the HLS-Ⅱ storage ring, which means that an additional quadrupole family may be necessary to reduce the perturbation from the elliptically polarizing undulator.

References

1 Helmut Wiedemann. Particle Accelerator Physics. Third Edition. Berlin: Springer-Verlag, 2007. 784

2 Ivanyan M, Martirosyan Y, Tsakanov V. Nucl. Instrum. Methods in Phys. Res. A, 2004, **531**: 651

3 BAI Zheng-He, WANG Lin, JIA Qi-Ka et al. Lattice Optimization for the HLS-Ⅱ Storage Ring. Chin. Phys. C (HEP & NP), to be published

4 JIA Qi-Ka. Design Consideration of New Insertion Devices of Hefei Light Source. In: Proc. of IPAC 2011. Spain: San Sebastian, 2011. 3284

5 Carlos A. Coello Coello, Gregorio Toscano Pulido, Maximino Salazar Lechuga. IEEE Trans. Evol. Comp., 2004, **8**(3): 256